Received: 20 December 2018 | Revised: 21 February 2019 | Accepted: 28 February 2019

DOI: 10.1002/sia.6643

RESEARCH ARTICLE

WILEY SURFACE and INTERFACE ANALYSIS

Structural and optical properties of novel CdSe nanoparticles produced via a facile synthetic route: Studies on the effects of cadmium sources

Sharon Kiprotich[1] | Francis B. Dejene[1] | Martin O. Onani[2]

[1] Department of Physics, University of the Free State, (QwaQwa campus), Phuthaditjhaba, South Africa

[2] Department of Chemistry, University of the Western Cape, Bellville, South Africa

Correspondence
Sharon Kiprotich, Department of Physics, University of the Free State, (QwaQwa campus), Private Bag X-13, Phuthaditjhaba, 9866, South Africa.
Email: kiprotichs@ufs.ac.za

Funding information
National Research Foundation, TESP (ESKOM)

We report on the successful synthesis of CdSe nanoparticles (NPs) via a facile aqueous approach. Investigation on the effects of various cadmium sources in the precursor solution on the CdSe NPs is discussed. The structural and morphological properties characterized by the X-ray diffraction (XRD) and scanning electron microscope (SEM) displayed good features of the as-prepared CdSe NPs. The XRD pattern displayed a pure zinc blende crystal structure for all samples, with the most crystalline sample observed for CdSe NPs prepared using anhydrous cadmium chloride. The estimated crystallite sizes were below 6 nm for all the CdSe NPs samples. Mixed shapes of spherical and nanorods of varying sizes were observed from the SEM images for the as-prepared NPs prepared using different cadmium sources. The optical studies conducted by photo-spectroscopy pointed out the CdSe NPs prepared using anhydrous cadmium chloride gave the best optical properties. The emission wavelengths were in the range 565 to 574 nm while the optical band gaps were in the range 2.94 to 3.23 eV for all the as-prepared CdSe NPs samples. All the samples, however, displayed quantum confinement effects giving room for further fabrication and engineering to suit specific applications in the biological field. The obtained results demonstrated that aqueous phase synthetic route employed in this study could be successfully adopted for production of high-quality CdSe NPs because of its facile and inexpensive nature.

KEYWORDS

CdSe nanoparticles, morphology, particle size, photoluminescence, structural properties

1 | INTRODUCTION

The unique optical properties of semiconducting nanoparticles (NPs) are the key factors that have attracted great interest of many nanotechnologists and material scientists all over the world. The band gap energy is the main optical property of semiconductor NPs. The technology of nanoscience has increased the understanding of the basic properties and possible applications of various nanomaterials and has stimulated interest in the study of metal selenide NPs. This is because the nanomaterials have promising ideas on the fundamental principles of physics and chemistry, which explains the great attraction of practitioners from various disciplines to the field of nanoscience and nanotechnology.[1] This nanotechnology has motivated the shift from the macroscopic to nanoscopic world due to the evolution of unique material properties and the changes that occur on the surface of the material. This is a phenomenon referred to as quantum size effects. This transition forms a vital aspect of the science of nanomaterials because in the macroscopic materials, majority of the atoms are hidden in the bulk of the material. When materials have reduced sizes and large surface area-to-volume ratios, they possess

distinctive optical, electronic, catalytic, and magnetic properties.[2] The material properties of nanoscaled particles are known to depend on their shape, size, surface features, and other parameters such as dopants introduced into the material when they interact with the surrounding environment.[3-5]

In the recent past, CdSe NPs have drawn the attention of an enormous number of research scientists widely because of its applications in various fields such as lasers, solar cells, biological fluorescent labels, and light-emitting diodes.[6-8] In an attempt to achieve these ends, there are factors that need to be considered during the preparation of these CdSe NPs. Some of the key issues to consider are the novelty, speed of production, cost of production, and their ability to be produced in large scale. Furthermore, the choice of method of preparation should be able to produce CdSe NPs of high quality with desired material properties. Various approaches have been used to synthesize these CdSe NPs by many researchers. These synthetic routes include the solvothermal route, sonochemical route, single molecule precursor route, microwave irradiation route, non-organometallic precursor route, and organometallic precursor route.[9-14] Murray et al[13] developed the organometallic route where they utilized a cadmium precursor $Cd(CH_3)_2$ source with a Se precursor. The cadmium source turned out to be pyrophoric, expensive, and hazardous.[15-17] Yu and Peng[16] managed to come up with a simpler non-organometallic route using CdO as cadmium precursor source, which is inexpensive and less toxic. The use of coordinating and noncoordinating solvents such as octadecene (ODE) and trioctylphosphine oxide (TOPO) has been studied extensively[16,17] where the reaction involve the use of solvents TOPO (or ODE), the Cd solution, and the trioctylphosphine (TOP-Se) solution. Although this route produce good quality CdSe NPs, it is slightly expensive and requires inert atmosphere and high boiling temperatures.

Despite the fact that the CdSe NPs produced from organic solvent synthetic routes at high temperatures possess good properties such as good monodispersion as displayed by narrow photoluminescence (PL) emission full width at half maximum (FWHM), wide range of emission colours (300-2500 nm) obtained by simply tuning the size, structure, and/or the composition,[15,16,18-21] the CdSe NPs produced are insoluble in water. Hence, this poses a challenge on how to make the as-prepared NPs soluble in water and also active in bioconjugate reactions.

The NPs applied in the biological field such as biomedical imaging, among others, have recently become one of the hottest research topics.[22-24] For biomedical applications, the NPs prepared need to be of high quality and soluble in water. The attempts made have shown that it is possible to prepare the NPs directly in water, though it produces NPs with wide size distribution with narrow sizes.[25-27]

Also, for biological applications, certain shapes and sizes are required, which dictates the ability to rationally tune the shape of CdSe NPs from spheres to rods and wires.[28,29] This is a great motivation in trying to produce CdSe NPs for a wide range of materials, including group II-VI, III-V, and IV semiconductors.

This study describes a facile synthetic route of preparing CdSe NPs for use in biological imaging. The reported route produces water-soluble CdSe NPs without performing complicated processes such as ligand exchange. The as-synthesized CdSe NPs were of zinc blende crystal structure with various morphologies obtained depending on the growth conditions and precursor solutions. The study further investigates the effects of cadmium source precursors on the as-grown CdSe NPs in detail. This is conducted in order to identify the right/convenient cadmium source to be used to grow high-quality CdSe with desired material properties for use in bio-imaging applications. This facile synthesis of CdSe NPs is of great interest because it provides a simpler, safer, more convenient, reliable, and eco-friendly route compared with many reported synthetic routes. Moreover, high-quality CdSe NPs are produced.

2 | EXPERIMENTAL PROCEDURE

The chemicals used in this experiment include cadmium sulphate hydrate (>99%), anhydrous cadmium acetate (>99%), anhydrous cadmium nitrate (>99%), anhydrous cadmium chloride (>99%), sodium sulphite (>98%), selenium powder (>99%), thioglycolic acid (TA) (>99%), and acetone (>99%). The chemicals were purchased from Sigma Aldrich and were used without any further purification.

The synthesis process was done in two steps as follows: In the first step, reduction of selenium was conducted by refluxing a mixture of 0.31 g of selenium and 1 g of sodium sulphite in 100 mL of deionized water (DI) for 6 hours at 80°C to form sodium selenosulphate. Se ions were obtained from the sodium selenosulphate prepared in step 1. In the second step, 0.2 mmol of cadmium chloride was dissolved in 50 mL of DI, and appropriate amounts of TA was added to form a molar ratio of TA/Cd of 1.4. The precursor pH was adjusted to basic medium, pH 11, as this favours the formation of uniformly dispersed NPs. The solution mixture was transferred to a 3-necked flask under stirring, and 3 mL of the reduced Se was added to the solution and refluxed for 1 hour at boiling temperature to form CdSe NPs. The CdSe NPs were then cooled down to room temperature, washed with excess acetone, and then dried to form the CdSe nanopowders. The above procedure was then repeated, but different cadmium sources S1, S2, S3, and S4 (S1-sulphate, S2-acetate, S3-nitrate, and S4-chloride) were used in the precursor to form CdSe NPs samples while all other parameters were kept constant in order to study the effects of cadmium sources on the growth of the CdSe NPs.

The crystal structures of the as-prepared CdSe NPs were characterized by using X-ray diffractometer (XRD) (a Phillips Advance Bruker D8) using CuKα radiation in the 2θ range from 20° to 80°. Scanning electron microscopy (SEM) images were obtained from JOEL electron microscope with X-ray dispersive spectroscope (EDS) attached to it to determine the elemental composition of the CdSe NPs. The optical studies were carried out using PL spectrophotometer containing a xenon lamp, which acts as the excitation source to measure emission spectra while ultraviolet visible (UV-Vis) evolution 1700 recorded the UV-Vis absorbance spectra.

3 | RESULTS AND DISCUSSION

3.1 | Formation mechanism of CdSe NPs

The CdSe NPs were synthesized via a facile route. A schematic diagram (Scheme 1) describes the growth mechanism of the CdSe NPs. The reaction between the Se powder and sodium sulphite allows the SO_3^{2-} ions to react with Se to form selenosulphate ($SeSO_3^{2-}$) ions (Equation 1). The $SeSO_3^{2-}$ ions are believed to react with the complexed cadmium chloride solution or any of the cadmium sources and used with TA to form CdSe NPs. The sodium selenosulphate releases the selenide ions gradually upon hydrolytic decomposition in alkaline media as the pH of the complexed cadmium precursor source is adjusted to pH of 11, which is a basic medium. The Se ions will then react with Cd^{2+} ions by the mechanism described by Ma et al.[30] This process is described by Equation 2.

The cadmium chloride or any of the other cadmium precursor source used reacts with the complexing agent, the TA, to form the Cd complex. This is followed by the Cd complex reacting with reduced Se under reflux at boiling temperature to form CdSe NPs. Possible reactions involved is shown in Scheme 1, which is then summarized in the redox chemical equations (Eq.) in Equations 1 and 2 to form the CdSe NPs.

$$SO_3^{2-} + Se \rightarrow SeSO_3^{2-}, \quad (1)$$

$$Cd^{2+} + SeSO_3^{2-} + 2OH^- \rightarrow CdSe + SO_4^{2-} + H_2O. \quad (2)$$

Various cadmium precursor sources were used to perform the investigations in this report. Different cadmium precursor sources release cadmium ions at different rates thus causing variation in the formation mechanism of CdSe NPs resulting in the CdSe NPs with various structural and optical properties. The effects of these cadmium precursor sources can be observed when all other growth parameters are kept constant during the entire growth process.

3.2 | Structural, morphological, and compositional analysis

3.2.1 | XRD analysis

The CdSe NPs synthesized via the aqueous route were found to possess crystal structure different from those produced through the organometallic method. The XRD pattern of CdSe NPs using different cadmium precursors is presented in Figure 1. All the as-prepared samples had characteristic features that correspond well to the bulk zinc blende crystal structure pattern of CdSe. There are three distinct features in the XRD patterns occurring at the neighbourhood of 25°, 41°, and 49° of diffraction angles, which match well with the (111), (220), and (311) planes of JCPDS No. 19-0191 zinc blende bulk CdSe. The S1, S3, and S4 display a high level of purity because of the absence of extra diffraction peaks, which could be from impurities in the sample such as in the S2 sample. These clearly indicate the dependence of the CdSe NPs formation on the cadmium source precursors. The diffraction peaks of the as-obtained samples were broad, an indication of extremely small particles formed that have features that deviate much more from the bulk crystalline structures. The XRD patterns for all the samples are similar except for the centre position, the FWHM, and reflection peak intensities, which are brought about by the different cadmium source used during the growth process. It was found that S4 sample prepared using cadmium chloride as the cadmium source presented the most crystalline sample as displayed by the most intense diffraction peaks. The crystallite sizes of the CdSe NPs were estimated using Debye-Scherrer formula[31] in Equation 3:

$$S = \frac{0.9\lambda}{\beta cos\theta}, \quad (3)$$

where S is the crystallite size, λ is the wavelength of CuKα radiation (1.5406 Å), θ is the Bragg's diffraction angle, and β is the broadening of the diffraction line FWHM. The obtained values were found to vary with the different cadmium sources used in the experiment. The variations in the sizes of the crystallites in the as-prepared CdSe NPs are due to changes in the lattice parameters, which are a result of growth of the NPs and contributions made by internal microstrain experienced by the NPs during growth (Table 1).

Different cadmium sources cause the CdSe NPs to grow in different ways especially at nucleation stage where the Cd complexes

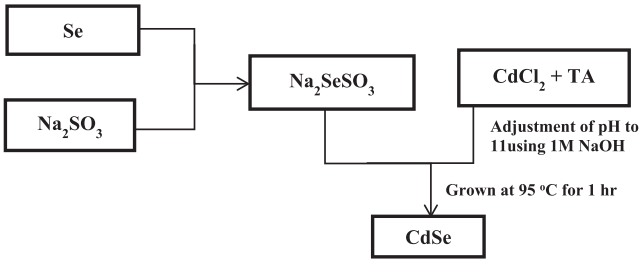

SCHEME 1 A schematic diagram showing the formation of CdSe nanoparticles (NPs)

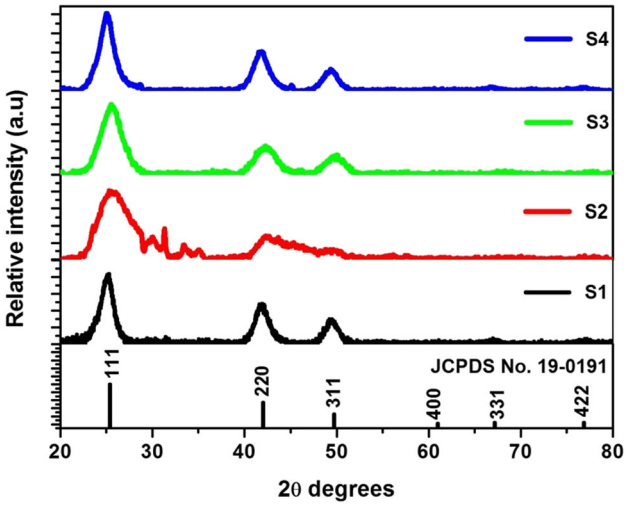

FIGURE 1 A graph displaying the CdSe nanoparticles (NPs) X-ray diffraction (XRD) pattern prepared using different cadmium sources

TABLE 1 Detailed values of various parameters calculated from the X-ray diffraction (XRD) pattern of different CdSe nanoparticle (NP) samples prepared using different cadmium sources

XRD Analysis						
Sample	**Plane**	**2θ**	**Peak Intensity, a.u**	**FWHM**	**Crystallite Size, nm**	**Average Crystallite, nm**
S1	111	25.059	707.29	1.4658	5.551	5.723
	220	41.892	416.88	1.5106	5.631	
	311	49.469	253.17	1.4611	5.986	
S2	111	25.896	676.16	3.0997	2.631	3.276
	220	43.345	156.19	3.0466	2.806	
	311	49.397	87.21	1.9904	4.393	
S3	111	25.554	757.24	2.3081	3.529	3.726
	220	42.299	308.55	2.2853	3.727	
	311	49.824	210.36	2.2341	3.921	
S4	111	25.046	1754.51	1.6164	5.034	5.121
	220	41.801	918.41	1.6755	5.075	
	311	49.332	510.22	1.6644	5.252	

Abbreviation: FWHM, full width at half maximum.

are released to the growth solution at different rates depending on the cadmium source. Also, the production of well-complexed Cd^{+} ions and CdSe NPs vary with different cadmium sources. This leads to agglomeration of the as-prepared CdSe NPs as observed in the SEM images thus promoting Ostwald ripening process to take place in the NPs, and hence, the growth of the NPs.[32] All these contributing factors led to different FWHM and crystallite size values obtained in this study. The lattice parameters and d-spacing of the CdSe cubic crystal structure prepared using different cadmium sources were calculated by guidance of the Bragg's law for the three distinct planes (111), (220), and (311) of the obtained XRD patterns, and the results were tabulated in Table 2. There was slight variation in the values of the lattice parameters with the use of different cadmium sources. The obtained values were also observed to deviate from the standard bulk values of 0.3428, 0.2099, and 0.1790 nm for the d-spacing and 5.937 Å for lattice parameters $a = b = c$ for diffraction planes (111), (220), and (311), respectively. This deviation is an indication of the presence of internal strain in the samples. The values of strain were estimated[33] using Equation 4:

$$\varepsilon = \frac{\beta}{4\tan\theta}, \tag{4}$$

where θ is the diffraction angle and β is the full width at half maximum. The calculated values are shown in Table 2.

The length of the dislodgment streaks per unit volume, commonly known as the dislocation density (δ), was calculated using the following equation (Equation 5) suggested by Velumani and Sharma et al.[34,35]:

$$\delta = \frac{1}{D^2}, \tag{5}$$

where D is the size of the crystal obtained from the XRD pattern as explained earlier. The calculated values of the dislocation density were 0.0306, 0.093, 0.0719, and 0.0381 lines/nm^3 for S1, S2, S3, and S4, respectively. Since this dislocation density is an indicator of the

TABLE 2 The calculated values of the lattice parameters obtained from the X-ray diffraction (XRD) pattern for CdSe nanoparticle (NP) samples prepared using different cadmium sources

Lattice Parameters and Strain						
Sample	**Plane**	**d-Spacing, nm**	**a, Å**	**Average a, Å**	**Average Strain (ε), lines/nm^2**	**Dislocation Density (δ), lines/nm^3**
S1	111	0.3551	6.151	6.117	1.142	
	220	0.2155	6.095			0.0306
	311	0.1841	6.106			
S2	111	0.3438	5.955	5.989	2.122	
	220	0.2086	5.901			0.0930
	311	0.1843	6.113			
S3	111	0.3483	6.033	6.046	1.867	
	220	0.2135	6.039			0.0719
	311	0.1829	6.066			
S4	111	0.3553	6.154	6.128	1.273	
	220	0.2159	6.107			0.0381
	311	0.1846	6.122			

dislocation network in the particle structure, the decrease in the dislocation density designates improved crystallinity.[35]

3.2.2 | SEM images

Morphological and composition analyses were conducted using the SEM. The obtained results displayed the formation of nanorods features on the samples of different sizes and orientation. Use of various cadmium sources in the preparation of CdSe NPs cause the production of different surface morphologies. Figure 2A shows the SEM images of the as-prepared CdSe NPs prepared using different cadmium sources in the precursor solution. In all the samples, spherical and rod-like particles are observed. S1 and S4 CdSe samples prepared from anhydrous cadmium phosphate and cadmium chloride showed morphologies that are composed of spherical and rod NPs. The spherical NPs are seen in agglomerated form appearing in groups. S2 sample formed using cadmium acetate displayed both nanorods and spherical NPs. The spherical NPs in the S2 sample agglomerate to form oval-like and rod-like features. The anhydrous cadmium nitrate used as cadmium source to prepare S3 sample produced CdSe nanorods, which are densely packed and uniformly distributed over the entire surface. The rod-like NPs in S4 have been affected by aggregation, thus forming blade-like shapes on the surface. These results show that the cadmium sources used to prepare the CdSe NPs impact greatly on the surface morphology of the as-prepared NPs. Hence, attention must be put in the choice of the cadmium source to be used especially in designing the CdSe NPs for certain application. This is because different types of morphologies act differently in various applications.

The elemental composition was conducted using EDS, and the spectra are shown in Figure 2B. The obtained results confirmed the presence of the expected elements in a fair stoichiometric ratio. This is supported by the atomic percentages calculated from the EDS spectra. The obtained atomic percentages of Cd and Se were (61.3, 38.7), (56.6, 43.4), (57, 43), and (53.3, 46.7) for S1, S2, S3, and S4, respectively. From the calculated results, it is clearly seen that all the cadmium sources produced cadmium-rich CdSe NPs, with S4 showing a fairer stoichiometric ratio compared with the other samples. This shows that different cadmium sources produce varying Cd:Se atomic ratios. Cadmium chloride was found to be a better cadmium source to grow CdSe with a ratio close to 1:1 with enhanced crystal qualities as displayed by highest diffraction peak intensities from XRD analysis.

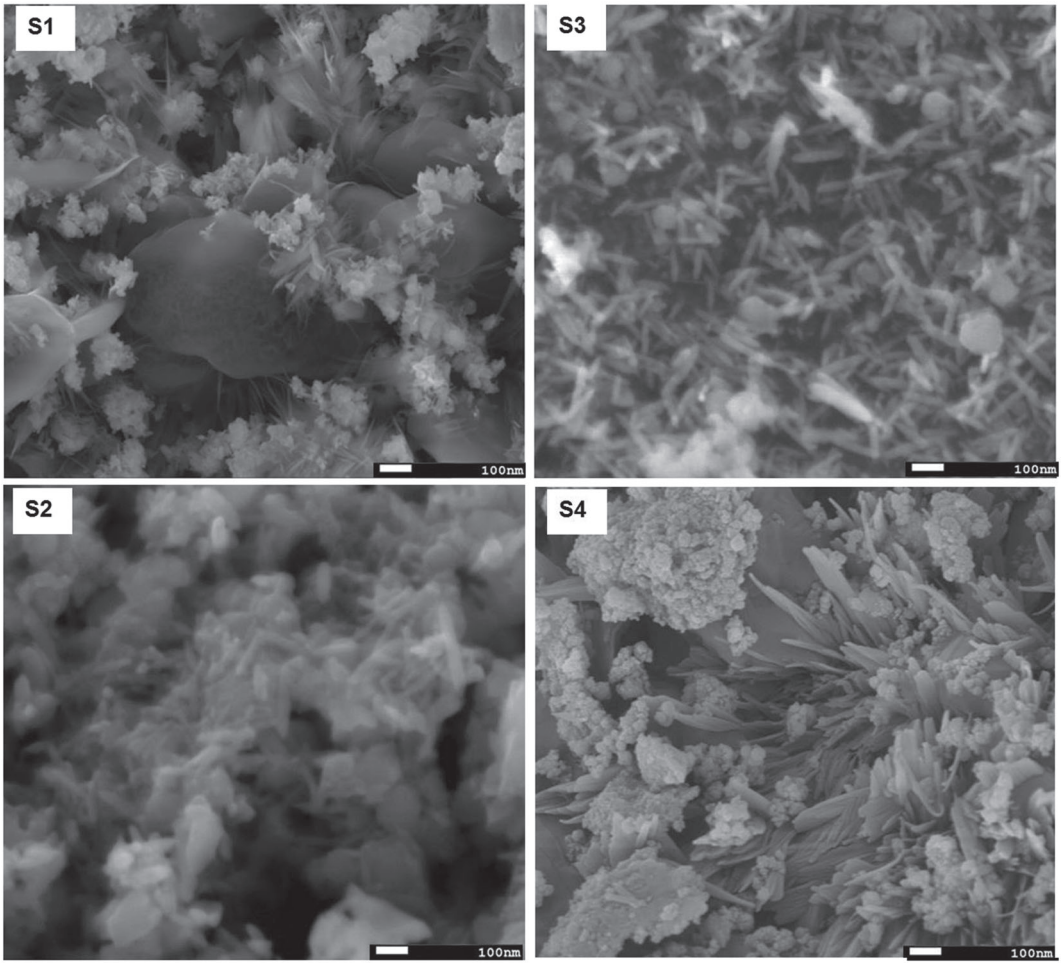

FIGURE 2 A, Micrographs displaying the scanning electron microscopy (SEM) images representing CdSe nanoparticles (NPs) prepared using different cadmium sources. B, Energy-dispersive X-ray spectroscopy (EDS) spectrum of CdSe NPs prepared using different cadmium sources

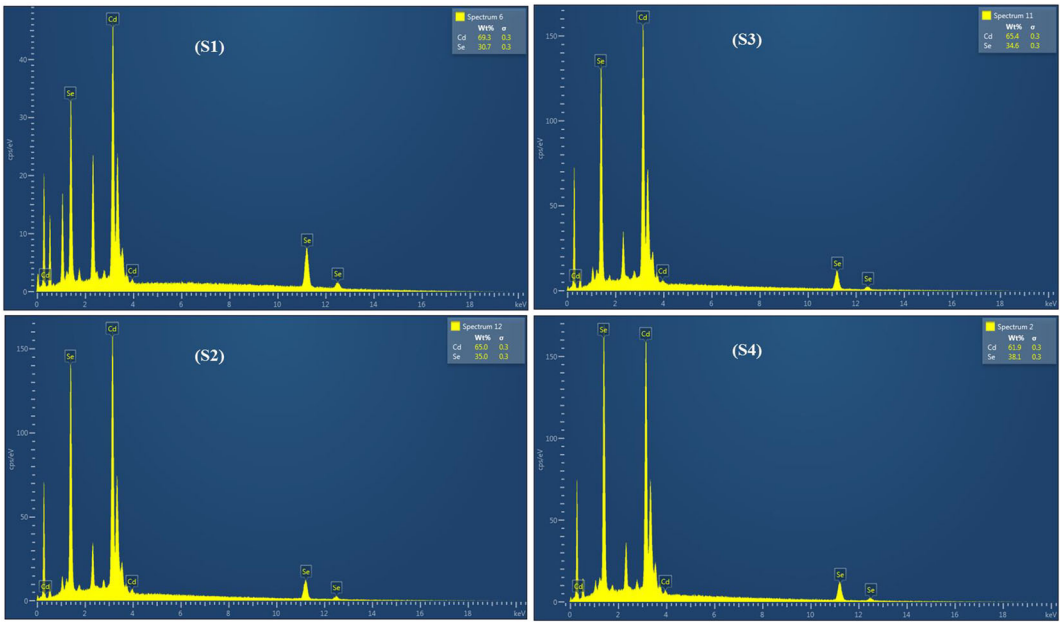

FIGURE 2 Continued.

3.3 | Optical properties

3.3.1 | PL analysis

Figure 3A displays the development of the PL emission spectra of the as-prepared CdSe NPs measured at room temperature using excitation wavelength of 400 nm. The spectra show the formation of an almost asymmetric pattern with defined emission bands for the different cadmium source samples. Considering the shape and peak position, these obtained PL characteristics can be ascribed to the exciton recombination localized at various surface states with relatively low energies.[36]

The PL peak position and intensity varied with the use of the different cadmium sources. The longest emission wavelength was obtained when anhydrous cadmium acetate (S2) was used, while anhydrous cadmium nitrate sample (S3) emitted the shortest wavelength. The longest emission wavelength observed from the S2 sample could be due to defects caused by the largest strain value as observed in the XRD analysis, and, also, it could be attributed to the large particle size as shown by the smallest band gap and particle estimation by effective mass approximation (EMA) (Table 3). The PL emission parameters are shown in Table. 3. However, the CdSe NPs with highest emission brightness is the one prepared using anhydrous cadmium chloride (S4) as depicted by the highest PL emission intensity compared with the other samples. The PL spectra of as-prepared CdSe NPs displayed good features that are similar to the best features of these CdSe NPs prepared using other approaches with high boiling solvents such as TOP.[16,37]

The values of PL FWHM were analysed and found to be in the range of 47 to 67 nm for all the CdSe NPs samples prepared. The narrowest FWHM was observed in the S4 sample (Table. 3), which also portrays the highest emission intensity. The sharp narrow and most intense peak observed for the S4 sample can be attributed to the high stability of the cadmium precursor and improved crystallinity of the sample.[38]

The Stoke shifts of the samples S1, S2, S3, and S4 were 60.9, 59.4, 62.2, and 63.7 nm, respectively. The enhanced Stoke shift observed in S4 with increase in the aspect ratio of the CdSe nanorods was found to be consistent with the expectations of the nanorods as explained by Hu et al[39] and Shabaev and Efros.[40] Figure 3B shows the Commission International de l'Eclairage (CIE) diagram displaying the colours of the PL emission.

The colour coordinates in the CIE map shown in Figure 3B depict clearly that the emission colours of the as-prepared CdSe NPs samples grown using various cadmium precursors all fall in the yellow-orange region of the CIE map. These results are in good agreement with results obtained from the PL measurement. Furthermore, it also confirms the fact that different cadmium sources used in the precursor solution have an impact in the size of the NPs formed, which in turn influences the colour and intensity of the emission produced.

3.3.2 | Absorbance analysis

The absorption spectra obtained from the UV-Vis spectrophotometer was used to study the progressive growth of the size and size distribution of CdSe NPs prepared by the reported facile synthetic route. The small solutions of each sample were used to measure the absorbance of as-prepared NPs. Figure 4A shows the absorption spectra of the as-prepared CdSe NPs prepared using different cadmium sources. From the absorption spectra, it can be deduced that the sizes of the CdSe NPs are closely monodisperse because of the presence of the absorption peak if the growth stops at size focusing regime as suggested by Peng and Peng.[15] The absorption edges are observed to vary with

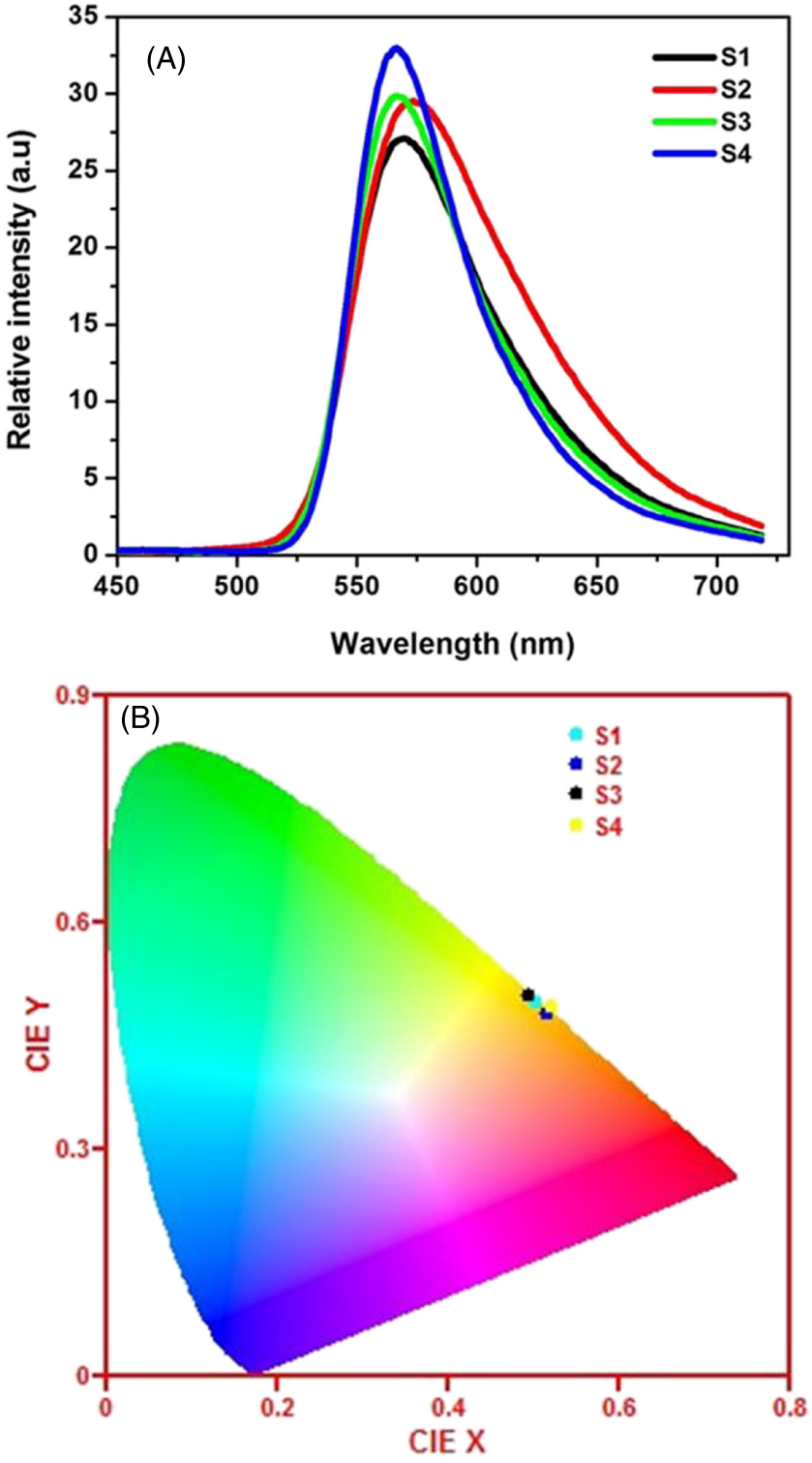

FIGURE 3 A, Photoluminescence (PL) spectra of the as-prepared CdSe nanoparticles (NPs) synthesized using different cadmium sources. B, A Commission International de l'Eclairage (CIE) chromaticity diagram showing the emission colours of the CdSe NPs prepared using different cadmium sources

different cadmium sources. The shapes of the absorption spectra are similar showing that all the cadmium sources used are capable of producing the CdSe NPs of certain properties only if all other parameters such as pH, reaction time, and reaction temperature are optimized. All the data obtained from these spectra are tabulated in Table 3 for comparison. Figure 4A was used to obtain the absorption maxima of the as-prepared CdSe NRs, which was then used to estimate the particle size using Equation 6 invented by Yu et al[41]:

$$S = \left(1.6122 \times 10^{-9}\right)\lambda^4 - \left(2.6575 \times 10^{-6}\right)\lambda^3 + \left(1.6242 \times 10^{-3}\right)\lambda^2 - (0.4277)\lambda + (41.57), \quad (6)$$

where S is the particle diameter and λ is the wavelength of the first absorption maximum obtained from the absorbance spectra. The approximated values were in close agreement to the values obtained from other techniques on the size of the CdSe NPs. Figure 4A was

TABLE 3 Optical parameters obtained from the photoluminescence (PL) emission and absorbance spectra of CdSe nanoparticles (NPs) prepared using various cadmium sources

	PL Emission Properties			UV-Vis Properties		
Sample	Peak Wavelength, nm	Peak Intensity, a.u	FWHM	Absorption peak, nm	Band gap energy, eV	Particle Size by EMA, nm
S1	569.1	27.1	57.94	630	3.12	3.29
S2	574.6	29.6	67.77	634	2.94	3.53
S3	565.8	30.1	53.05	628	3.21	3.19
S4	566.3	33.2	47.76	630	3.17	3.23

Abbreviations: EMA, effective mass approximation; FWHM, full width at half maximum: UV-Vis, ultraviolet visible.

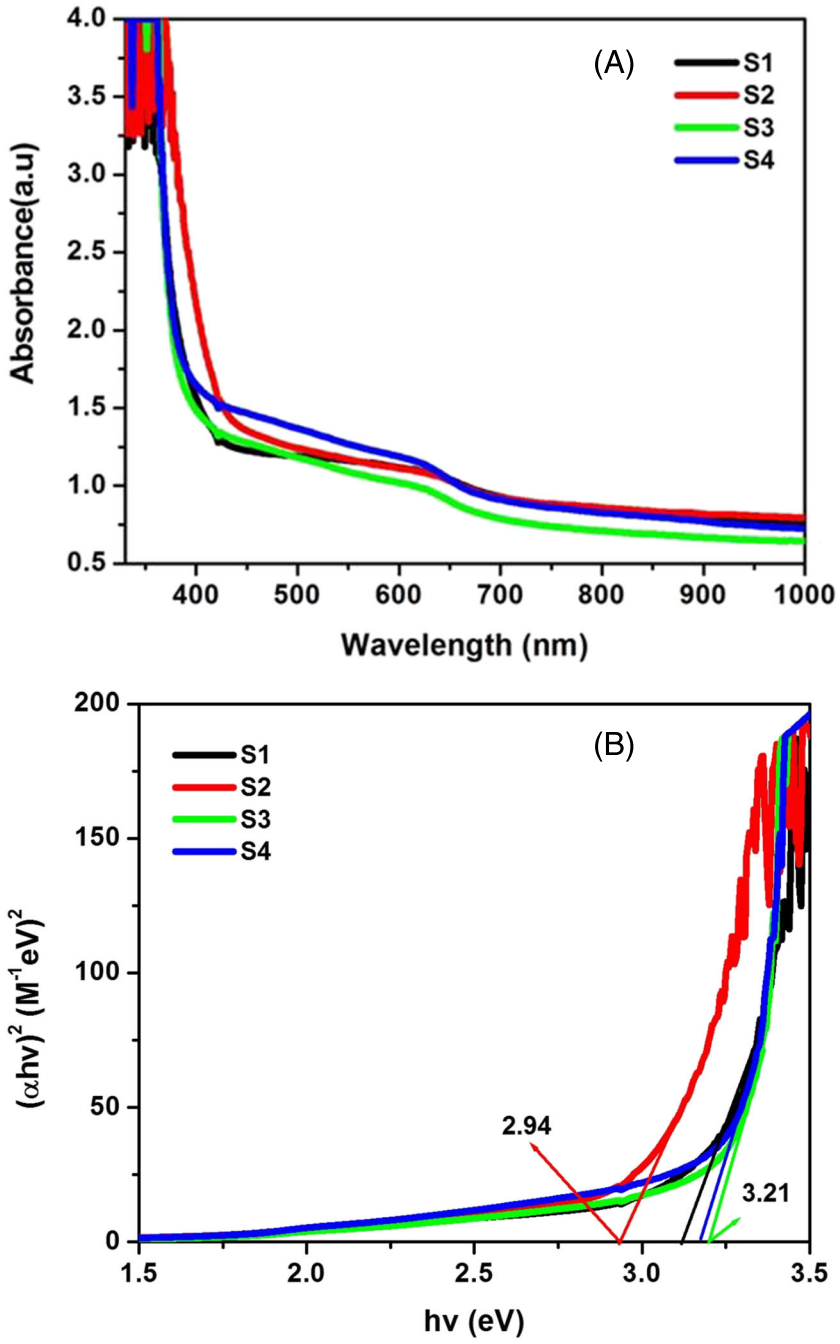

FIGURE 4 A, Absorption spectra of the CdSe nanoparticles (NPs) prepared using different cadmium sources. B, Graphs showing Tauc plots used to estimate the band gap energies of the CdSe NPs prepared using different cadmium sources

used to calculate the band gap energies of the as-prepared CdSe NPs using the common Tauc's equation (Equation 7)[42]:

$$\frac{\alpha = (hv - E_g)^n A}{hv}, \tag{7}$$

where A is a constant (free of photon energy) and is directly related to the measured absorbance, E_g is the energy band gap of the prepared sample, α is the absorption coeffecient, and the parameter that characterizes the transition process is represented by the exponent. The absorption coefficient was calculated using the famous Beer-Lambert relation[43] in Equation 8:

$$\alpha = \frac{A}{LC}, \tag{8}$$

where A is the absorbance, L is the thickness of the cuvette used to take the measurements, and C is the concentration of the solution.

Since the absorption coeffecient is directly related to the measured absorbance, in cases where other parameters used to calculate the absorption coeffecient are not there, the square of absorbance can be used in the approximation. By doing this, there is negligible error observed in the obtained optical band gap energies of the CdSe NPs prepared. The Tauc plots were drawn and the straight part of the graphs extrapolated to the energy axis and the values of the optical band gap recorded. The estimated band gap values were tabulated in Table 3 for different CdSe NPs prepared using various cadmium sources. The realized values are larger than the reported bulk band gap[44] 1.74 eV because of the quantum confinement effects observed from the as-grown CdSe NPs. The absorption transitions are from band to band while the PL emissions are from donor to band. If the PL emission is in the UV region, then to calculate the band gap from PL, the difference between the donor and conduction band for CdSe must be added. The PL emissions under study are defects emissions, hence cannot be used for band gap calculations. However, if PL emission positions are used to estimate band gap at a glance, the obtained values are 2.179, 2.161, 2.191, and 2.189 eV. These values also portray the quantum confinement effects but slightly smaller than the one estimated from the Tauc's relation. This is because the Tauc's relation gives a more accurate value than the estimated values from emission wavelength.

As shown in Table 3, the estimated size range of CdSe NPs was approximately less than 5 nm. These values indicate the presence of quantum confinement in the samples, and therefore a simple EMA model proposed by Brus[45] can be used to estimate the size of the CdSe NPs obtained. This is performed because of the fact that from observation, it is quite clear that the estimated band gap energies are larger than the value of the bulk CdSe band gap, which points to the sizes being in the regime of spatial exciton confinement, which makes it possible to estimate the average particle radius using the effective mass approximation method (EMA)[46] by Equation 9:

$$\Delta E_g = \frac{\hbar^2 \pi^2}{2S^2}\left(\frac{1}{M_e^*} + \frac{1}{M_h^*}\right), \tag{9}$$

where ΔE_g is the difference between the energy band gap of the material under study and the bulk band gap, S is the particle Bohr radius while M_e^* and M_h^* are effective masses of electron and hole respectively. The M_e^* and M_h^* values[47,48] for CdSe used were $0.13m_0$ and $0.45m_0$, where m_0 is the electron/hole rest mass.

4 | CONCLUSION

This study demonstrates clearly that stable CdSe NPs with well-defined amounts of fundamental atoms can be easily fabricated via a facile aqueous technique. This is because the CdSe NPs were synthesized at low temperature in an open air condition. Various techniques were employed to characterize the material properties of the obtained CdSe NPs in order to study the effects of various cadmium sources on these CdSe NPs. The CdSe NPs exhibited zinc blende crystal structure in all the samples, with the most crystalline sample observed when anhydrous cadmium chloride was used in the precursor solution. The CdSe NPs displayed relatively sharp excitonic PL emission, with S4 having the smallest PL FWHM, which is due to monodispersed size distribution. The optical band gaps of all the CdSe NPs samples prepared displayed the presence of the quantum confinement effects as depicted by the large energy values compared **with** the bulk band gap value. The difference observed in the material properties of the CdSe NPs is attributed to the variation in the reactivity of the different cadmium precursor used during synthesis. Our current results therefore should be a very significant step towards a convenient, reliable, economical, safe, and eco-friendly fabrication of high-quality semiconductor NPs for bio-imaging applications. Anhydrous cadmium chloride is recommended for fabrication of the CdSe NPs using the reported synthetic approach as this produces highly crystalline and well-dispersed NPs in the quantum confinement regime. This further allows for further fabrication and engineering of the NPs for a specific biological application.

ACKNOWLEDGEMENTS

The authors wish to acknowledge the financial support for this project from National Research Foundation, TESP (ESKOM).

ORCID

Sharon Kiprotich https://orcid.org/0000-0002-7941-5449

REFERENCES

1. Shoair AGF. Ultrasonic-assisted ruthenium-catalyzed oxidation of some organic compounds in aqueous medium. *J Mol Liq*. 2015;206:68-74.
2. Marcial MM, Pleixats R. Formation of carbon-carbon bonds under catalysis by transition-metal nanoparticles. *Acc Chem Res*. 2003;36(8):638-643.
3. Jayanthi K, Chawla S, Chander H, Haranath D. Structural, optical and photoluminescence properties of ZnS: Cu nanoparticle thin films as a function of dopant concentration and quantum confinement effect. *Cryst Res Technol*. 2007;42(10):976-982.

4. Ramamurthy N, Kumar MR, Murugadoss G. Synthesis and study of optical properties of CdS nanoparticles using effective surfactants. *Nanosci Nanotechnol Int J*. 2011;1(3):12-16.
5. Chan WCW, Nie S. Quantum dot bioconjugates for ultrasensitive nonisotopic detection. *Science*. 1998;281(5385):2016-2018.
6. Colvin VL, Schlamp MC, Alivisatos AP. Light-emitting diodes made from cadmium selenide nanocrystals and a semiconducting polymer. *Nature*. 1994;370(6488):354-357.
7. Klimov VI, Mikhailovsky AA, Xu S, et al. Optical gain and stimulated emission in nanocrystal quantum dots. *Science*. 2000;290(5490): 314-317.
8. Green M, O'Brien P. Recent advances in the preparation of semiconductors as isolated nanometric particles: new routes to quantum dots. *Chem Commun*. 1999;22:2235-2241.
9. Cumberland SL, Hanif KM, Javier A, et al. Inorganic clusters as single-source precursors for preparation of CdSe, ZnSe, and CdSe/ZnS nanomaterials. *Chem Mater*. 2002;14(4):1576-1584.
10. Crouch DJ, O'Brien P, Malik MA, Skabara PJ, Wright SP. A one-step synthesis of cadmium selenide quantum dots from a novel single source precursor. *Chem Commun*. 2003;(12):1454-1455.
11. Gautam UK, Rajamathi M, Meldrum F, Morgan P, Seshadri R. A solvothermal route to capped CdSe nanoparticles. *Chem Commun*. 2001;(7):629-630.
12. Ge JP, Li YD, Yang GQ. Mechanism of aqueous ultrasonic reaction: controlled synthesis, luminescence properties of amorphous cluster and nanocrystalline CdSe. *Chem Commun*. 2002;(17):1826-1827.
13. Murray CB, Norris DJ, Bawendi MG. Synthesis and characterization of nearly monodisperse CdE (E=sulfur, selenium, tellurium) semiconductor nanocrystallites. *J Am Chem Soc*. 1993;115(19): 8706-8715.
14. Hambrock J, Birkner A, Fischer RA. Synthesis of CdSe nanoparticles using various organometallic cadmium precursors. *Mater Chem*. 2001;11(12):3197-3201.
15. Peng ZA, Peng X. Formation of high-quality CdTe, CdSe, and CdS nanocrystals using CdO as precursor. *J Am Chem Soc*. 2001;123(1): 183-184.
16. Yu WW, Peng X. Formation of high-quality CdS and other II-VI semiconductor nanocrystals in non-coordinating solvents: tunable reactivity of monomers. *Angew Chem Int Ed*. 2002;41(13): 2368-2371.
17. Bullen CR, Mulvaney P. Nucleation and growth kinetics of CdSe nanocrystals in octadecene. *Nano Lett*. 2004;4(12):2303-2307.
18. Yu WW, Falkner JC, Shih BS, Colvin VL. Preparation and characterization of monodisperse PbSe semiconductor nanocrystals in a non-coordinating solvent. *Chem Mater*. 2004;16(17):3318-3322.
19. Bailey RE, Nie S. Alloyed semiconductor quantum dots: tuning the optical properties without changing the particle size. *J Am Chem Soc*. 2003;125(23):7100-7106.
20. Kim S, Lim YT, Soltesz EG, et al. Near-infrared fluorescent type II quantum dots for sentinel lymph node mapping. *Nat Biotechnol*. 2004;22(1):93-97.
21. Michalet X, Pinaud FF, Bentolila LA, et al. Quantum dots for live cells, in vivo imaging, and diagnostics. *Science*. 2005;307(5709):538-544.
22. Gao X, Chan WCW, Nie S. Quantum-dot nanocrystals for ultrasensitive biological labelling and multicolour optical encoding. *J Biomed Opt*. 2002;7(4):532-538.
23. Wu X, Liu H, Liu J, et al. Immunofluorescent labelling of cancer marker Her2 and other cellular targets with semiconductor quantum dots. *Nat Biotechnol*. 2003;21(1):41-46.
24. Eastman PS, Ruan W, Doctolero M, et al. Qdot nanobarcodes for multiplexed gene expression analysis. *Nano Lett*. 2006;6(5):1059-1064.
25. Wang Y, Tang Z, Correa-Duarte MA, et al. Mechanism of strong luminescence photoactivation of citrate-stabilized water-soluble nanoparticles with CdSe cores. *J Phys Chem B*. 2004;108(40):15461-15469.
26. Kho R, Torres-Martinez CL, Mehra RK. A simple colloidal synthesis for gram-quantity production of water-soluble ZnS nanocrystal powders. *J Colloid Interface Sci*. 2000;227(2):561-566.
27. Winter JO, Liu TY, Korgel BA, Schmidt CE. Recognition molecule directed interfacing between semiconductor quantum dots and nerve cells. *Adv Mater*. 2001;13(22):1673-1677.
28. Pena DJ, Mbindyo JKN, Carado AJ, et al. Template growth of photoconductive metal-CdSe-metal nanowires. *J Phys Chem B*. 2002;106(30):7458-7462.
29. Kovtyukhova NI, Kelley BK, Mallouk TE. Coaxially gated in-wire thin-film transistors made by template assembly. *J Am Chem Soc*. 2004;126(40):12738-12739.
30. Ma XD, Qian XF, Yin J, Xi HA, ZhuJ ZK. Preparation and characterisation of polyvinyl alcohol-capped CdSe nanoparticles at room temperature. *Colloid Interface Sci*. 2002;252(1):77-81.
31. Cullity BD. *Elements of X-ray Diffraction*. Massachusetts: A.W.P.C.; 1967.
32. Kiprotich S, Onani MO, Dejene FB. High luminescent L-cysteine capped CdTe quantum dots prepared at different reaction times. *Phys B Condens Matter*. 2018;535:202-210.
33. Ting SY, Chen PJ, Wang HC, et al. Crystallinity improvement of ZnO thin film on different buffer layers grown by MBE. *J Nanomater*. 2012;2012:6.
34. Velumani S, Mathew X, Sebastian PJ, Narayandass SK, Mangalaraj D. Structural and optical properties of hot wall deposited CdSe thin films. *Sol Energy Mater Sol Cells*. 2003;76(3):347-358.
35. Sharma K, Al-Kabbi AS, Saini GSS, Tripathi SK. Determination of dispersive optical constants of nanocrystalline CdSe (nc-CdSe) thin films. *Mater Res Bull*. 2012;47(6):1400-1406.
36. Lee JRI, Meulenberg RW, Hanif KM, et al. Experimental observation of quantum confinement in the conduction band of CdSe quantum dots. *Phys Rev Lett*. 2007;98:146803(1)–146803(4).
37. Nair PS, Fritz KP, Scholes GD. A multiple injection method for inserting kinetic control in the synthesis of CdSe nanorods. *Chem Commun*. 2004;(18):2084-2085.
38. Kudera S, Zanella M, Giannini C, et al. Sequential growth of magic-size CdSe nanocrystals. *Adv Mater*. 2007;19(4):548-552.
39. Hu J, Li L, Yang W, Manna L, Wang L, Alivisatos AP. Linearly polarized emission from colloidal semiconductor quantum rods. *Science*. 2001;292(5524):2060-2063.
40. Shabaev A, Efros AL. 1D exciton spectroscopy of semiconductor nanorods. *Nano Lett*. 2004;4(10):1821-1825.
41. Yu WW, Qu L, Guo W, Peng X. Experimental determination of the extinction coefficient of CdTe, CdSe, and CdS nanocrystals. *Chem Mater*. 2003;15(14):2854-2860.
42. Tauc J. Optical properties of amorphous semiconductors. In: *Amorphous and Liquid Semiconductors*. Boston, MA: Springer; 1974: 159-220.
43. Beer A. Determination of the absorption of red light in colored liquids. *Ann Phys Chem*. 86(1852):78-88.
44. Gaponenko SV. *Optical Properties of Semiconductor Nanocrystals*." 23. Cambridge university press; 1998.
45. Brus L. Electronic wave functions in semiconductor clusters: experiment and theory. *J Phys Chem*. 1986;90(12):2555-2560.

46. Kippeny T, Swafford LA, Rosenthal SJ. Semiconductor nanocrystals: a powerful visual aid for introducing the particle in a box. *J Chem Educ*. 2002;79(9):1094.

47. Cohen E, Sturge MD. Fluorescence line narrowing, localized exciton states, and spectral diffusion in the mixed semiconductor CdS_xSe_{1-x}. *Phys Rev B*. 1982;25(6):3828-3840.

48. Trallero-Giner C, Debernardi A, Cardona M, Menendez-Proupin E, Ekimov AI. Optical vibrons in CdSe dots and dispersion relation of the bulk material. *Phys Rev B*. 1998;57(8):4664-4669.

How to cite this article: Kiprotich S, Dejene FB, Onani MO. Structural and optical properties of novel CdSe nanoparticles produced via a facile synthetic route: Studies on the effects of cadmium sources. *Surf Interface Anal*. 2019;51:722–732. https://doi.org/10.1002/sia.6643